JOURNAL OF VIROLOGY, July 1997, p. 5639–5646
0022-538X/97/$04.00+0

Vol. 71, No. 7

The UL20 Gene Product of Pseudorabies Virus Functions in Virus Egress

WALTER FUCHS,[1] BARBARA G. KLUPP,[1] HARALD GRANZOW,[2] AND THOMAS C. METTENLEITER[1]*

Institutes of Molecular and Cellular Virology[1] and Diagnostic Virology,[2] Friedrich-Loeffler-Institutes, Federal Research Centre for Virus Diseases of Animals, D-17498 Insel Riems, Germany

Received 3 February 1997/Accepted 3 April 1997

The UL20 open reading frame is positionally conserved in different alphaherpesvirus genomes and is predicted to encode an integral membrane protein. A previously described UL20$^-$ mutant of herpes simplex virus type 1 (HSV-1) exhibited a defect in egress correlating with retention of virions in the perinuclear space (J. D. Baines, P. L. Ward, G. Campadelli-Fiume, and B. Roizman, J. Virol. 65:6414–6424, 1991). To analyze UL20 function in a related but different herpesvirus, we constructed a UL20$^-$ pseudorabies virus (PrV) mutant by insertional mutagenesis. Similar to HSV-1, UL20$^-$ PrV was found to be severely impaired in both cell-to-cell spread and release from cultured cells. The severity of this defect appeared to be cell type dependent, being more prominent in Vero than in human 143TK$^-$ cells. Surprisingly, electron microscopy revealed the retention of enveloped virus particles in cytoplasmic vesicles of Vero cells infected with UL20$^-$ PrV. This contrasts with the situation in the UL20$^-$ HSV-1 mutant, which accumulated virions in the perinuclear cisterna of Vero cells. Therefore, the UL20 gene products of PrV and HSV-1 appear to be involved in distinct steps of viral egress, acting in different intracellular compartments. This might be caused either by different functions of the UL20 proteins themselves or by generally different egress pathways of PrV and HSV-1 mediated by other viral gene products.

Pseudorabies virus (PrV; Suid herpesvirus 1) is the causative agent of Aujeszky's disease in pigs but is also highly pathogenic for most other mammals except higher primates and humans (25, 37). PrV belongs to the herpesvirus subfamily *Alphaherpesvirinae* (28), which encompasses important pathogens, including human herpes simplex virus types 1 and 2 (HSV-1 and HSV-2), varicella-zoster virus (VZV), bovine herpesvirus 1 (BHV-1), equine herpesvirus 1 (EHV-1), Marek's disease virus, and infectious laryngotracheitis virus. The double-stranded DNA genome of PrV is approximately 150 kbp in size and consists of a unique long (U_L) region and an invertible unique short (U_S) region, which is flanked by inverted repeat sequences (7). Although the PrV genome has not yet been sequenced completely, available data indicate that gene arrangement within the PrV genome is largely collinear to that found in the completely sequenced alphaherpesvirus genomes of HSV-1 (24), VZV (10), EHV-1 (31), and BHV-1 (30) with the exception of a large inversion in the U_L region (6, 13) encompassing the UL27 to UL44 genes. Compared to the prototypic genome isomer of HSV-1, which possesses an invertible U_L region, the PrV U_L genome region was found in opposite orientation, as were the U_L regions of EHV-1 and BHV-1.

Several years ago, we and others (12, 20) determined the nucleotide sequence of the PrV homologs of the UL20 and UL21 genes of HSV-1 (24) which were detected in a similar arrangement, followed by a putative origin of DNA replication (20), and the gH gene (19, 21). The UL20 and UL21 open reading frames (ORFs) are positionally conserved in other alphaherpesvirus genomes, as in VZV, EHV-1, and BHV-1 (10, 31, 33). The UL21 gene of PrV was previously shown to encode a nonessential capsid protein, whose absence impairs the efficiency of cleavage and encapsidation of newly synthesized viral DNA (12) and strongly reduces the in vivo virulence of PrV (22). The UL21 gene of HSV-1 was also shown to encode a virion protein, which is dispensable for virus propagation in vitro (4). In contrast, first attempts to delete the HSV-1 UL20 gene failed when performed in baby hamster kidney cells (23). Further experiments using human 143TK$^-$ cells succeeded in isolation of a UL20$^-$ HSV-1 recombinant (3). These results indicated a cell-type-dependent relevance of HSV-1 UL20 for viral replication, which was confirmed by propagation of UL20$^-$ HSV-1 on different cell lines (3). Electron microscopy of nonpermissive Vero cells infected with UL20$^-$ HSV-1 revealed a defect in egress of enveloped virions from the perinuclear cisterna, resulting in an accumulation of virions in the perinuclear space (1, 3). The UL20 gene product of HSV-1 was reported to represent a presumably nonglycosylated membrane protein, which is present in nuclear membranes and Golgi vesicles of infected cells, as well as in the envelope of purified virions (34). Although the overall homology of the HSV-1 protein to the predicted 161-amino-acid UL20 gene product of PrV amounts to only 33% of identical residues (20), the presence of multiple clusters of hydrophobic amino acids in both the HSV-1 (23) and PrV proteins indicates that the PrV UL20 protein might also be an intrinsic membrane constituent.

To assess whether UL20 function in a different alphaherpesvirus is identical to that found in HSV-1, we constructed and analyzed a UL20$^-$ PrV mutant. For inactivation of the PrV UL20 gene, a 3,791-bp *Bam*HI-*Sal*I subfragment of genomic *Bam*HI fragment 4 containing the PrV UL20 and UL21 genes (Fig. 1C) was cloned into plasmid TN-77 (5) to obtain plasmid pBS3.8. After removal of the original *Bam*HI site by fill-in reaction with Klenow polymerase and religation, a novel *Bam*HI site was created at codon 42 of the UL20 gene by *Pml*I digestion and linker addition. Into this site, a 3,493-bp *Sal*I-

* Corresponding author. Phone: 49-38351-7102. Fax: 49-38351-7151. E-mail: Thomas.C.Mettenleiter@rie.bfav.de.

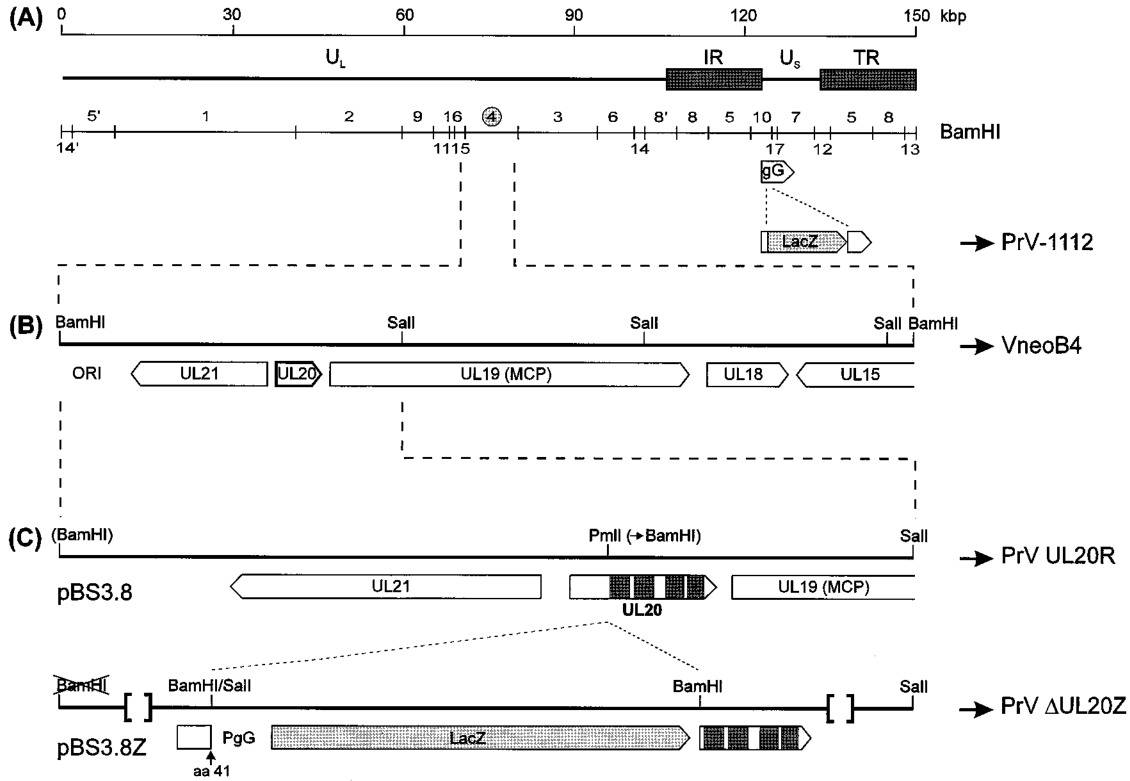

FIG. 1. Construction of UL20⁻ PrV. (A) The PrV genome consisting of a unique long (U_L) region and a unique short (U_S) region which is flanked by inverted internal (IR) and terminal (TR) repeat sequences. The *Bam*HI restriction fragment map of wild-type PrV and the *lacZ* insertion introduced in the glycoprotein G gene (gG) of mutant PrV-1112 are indicated. (B) Enlarged map of the 9.4-kbp *Bam*HI fragment 4, which contains the 3′-terminal part of the UL15 ORF; the entire UL18, UL19 (MCP, major capsid protein), UL20, and UL21 ORFs; and an origin of replication consensus sequence (ORI). *Bam*HI fragment 4 was used to establish the transcomplementing cell line VneoB4. (C) Plasmid pBS3.8 contains a 3,791-bp *Bam*HI-*Sal*I subfragment of *Bam*HI fragment 4, encompassing the UL21 and UL20 genes. After inactivation of the terminal *Bam*HI site (in parentheses), a novel *Bam*HI site was introduced by linker insertion mutagenesis of a *Pml*I site within the UL20 ORF. Into this site, the *lacZ* gene under control of the PrV gG gene promoter (PgG) was inserted as a *Sal*I-*Bam*HI fragment behind codon 41. The resulting plasmid, pBS3.8Z, was used to generate recombinant PrV ΔUL20Z. This virus mutant was rescued with plasmid pBS3.8 to obtain PrV UL20R. Clusters of hydrophobic amino acids representing putative transmembrane domains of the UL20 protein are shown as shaded boxes. Brackets indicate that the depicted DNA fragments are not drawn to scale. aa, amino acid.

*Bam*HI fragment encompassing a *lacZ* expression cassette (26) was inserted in parallel to the UL20 ORF by ligation of the compatible *Bam*HI sites, blunt ending of the noncompatible sites with Klenow polymerase, and ligation (Fig. 1C). Although this mutation does not prevent expression of the 5′-terminal part of the PrV UL20 gene, the resulting polypeptide, if stable at all, should hardly be functional since it lacks three-fourths of the original protein including the predicted membrane-spanning sequences (Fig. 1C). The resulting plasmid, pBS3.8Z, was cotransfected by calcium phosphate coprecipitation (16) with genomic DNA of PrV wild-type strain Ka (18) into Vero and VneoB4 cells. Vero-derived cell line VneoB4 (22) is stably transfected with a PrV genome fragment spanning the UL18 to UL21 ORFs (Fig. 1B). Virus progeny was screened for expected PrV recombinants by blue plaque assay (26) on VneoB4 cells. After cotransfection of normal Vero cells, no PrV recombinants could be isolated from progeny virus. In contrast, after cotransfection of VneoB4 cells, *lacZ*-expressing PrV recombinants could be detected and further plaque purified. VneoB4 cells complement PrV UL21 mutants in *trans* (22). As demonstrated here, mutation of the viral UL20 gene is also compensated in *trans* on this cell line, indicating that both the PrV UL20 and UL21 genes in cell line VneoB4 are functionally expressed after PrV infection. Since propagation of the PrV UL20 mutants on transcomplementing cells bears the risk of spontaneous rescue of the authentic viral UL20 gene by homologous recombination between viral and cellular DNA, the PrV UL20⁻ mutants were further plaque purified and propagated on noncomplementing MDBK cells, which supported replication of mutant virus reasonably well (see below). A randomly selected *lacZ*-expressing plaque isolate was further characterized and designated PrV ΔUL20Z. In order to generate an isogenic UL20 rescue mutant, virion DNA of PrV ΔUL20Z was cotransfected into normal Vero cells together with the cloned 3.8-kbp *Bam*HI-*Sal*I fragment of wild-type PrV DNA (Fig. 1C). Plaque assays of virus progeny were again performed on Vero cells, and wild-type-sized colorless PrV plaques were isolated after Bluo-Gal agarose overlay. A single plaque isolate, designated PrV UL20R, was further analyzed.

To ascertain the correct genotype of the UL20⁻ and UL20 rescue mutants, virion DNA of PrV ΔUL20Z and UL20R was compared to wild-type PrV DNA by *Bam*HI restriction analysis and Southern blot hybridization. As a consequence of an additional *Bam*HI site introduced at the 3′ end of the *lacZ* insertion within the UL20 gene (Fig. 1C), the PrV ΔUL20Z genome showed two novel 6.1- and 6.8-kbp *Bam*HI fragments instead of the 9.4-kbp *Bam*HI fragment 4 of wild-type PrV. In the UL20 rescue mutant, PrV UL20R, the wild-type genomic *Bam*HI fragment 4 was restored. Neither of the PrV mutants exhibited other than the expected alterations of the *Bam*HI

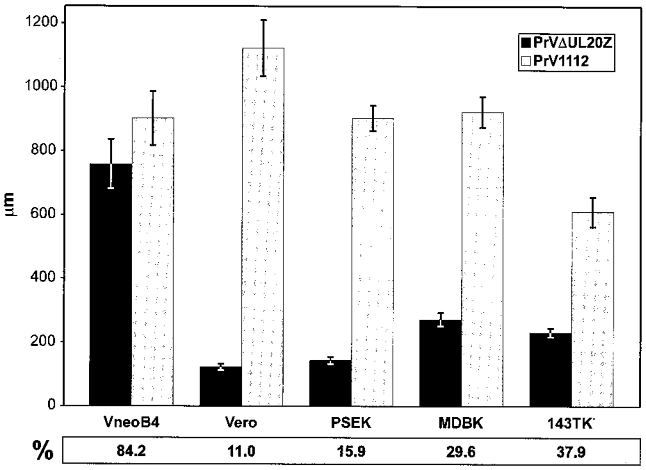

FIG. 2. Plaque size of UL20⁻ PrV. Vero, VneoB4, PSEK, MDBK, and 143TK⁻ cells were infected with either PrV ΔUL20Z or PrV-1112 under plaque assay conditions. Three days after infection, the average diameters of 30 X-Gal-stained plaques per virus and cell line were determined (bars). Standard deviations are indicated by vertical lines. The relative sizes of PrV ΔUL20Z versus PrV-1112 plaques are indicated below (%).

restriction patterns compared to wild-type PrV DNA (data not shown).

The in vitro phenotype of HSV-1 UL20 mutants is highly cell type dependent (3). To investigate whether this is also true for UL20⁻ PrV, plaque assays on Vero, VneoB4, porcine (PSEK) and bovine (MDBK) kidney, and human 143TK⁻ cells were performed. On most of these cell lines, PrV ΔUL20Z produced only very small plaques, which could be clearly detected only by X-Gal (5-bromo-4-chloro-3-indolyl-β-D-galactopyranoside) staining. To permit a similar staining of the wild-type control virus, PrV-1112 (26), which carries the *lacZ* gene within the nonessential glycoprotein G gene locus (Fig. 1A) and exhibits no growth defect in vitro or in vivo compared to wild-type PrV, was used (2, 27). Serial dilutions of PrV-1112 and PrV ΔUL20Z were plated in parallel onto cell monolayers, and cells were overlaid with medium containing 0.8% methylcellulose. After incubation for 3 days at 37°C, the cells were fixed and stained with X-Gal (29). Diameters of 30 randomly selected plaques per virus and cell line were measured microscopically, and average plaque sizes as well as standard deviations were determined (Fig. 2, upper panel). In addition to plaque diameters, the relative sizes of PrV ΔUL20Z plaques compared to that of PrV-1112 were calculated for each cell line (Fig. 2, lower panel). On Vero cells, plaque diameters of PrV ΔUL20Z amounted to only 11% of the wild-type size, indicating that mutation of the UL20 gene impairs cell-to-cell spread of PrV. This defect was complemented in *trans* on Vero cell line VneoB4, which harbors the intact UL20 gene. In these cells, plaque diameters of PrV ΔUL20Z were restored to more than 84% of the wild-type size. Significant growth deficiencies of UL20⁻ PrV were also detected on other noncomplementing cells, but to a lesser extent. On noncomplementing cells, the largest plaques of PrV ΔUL20Z were produced on MDBK cells. However, the smallest relative difference in plaque size of UL20⁻ PrV compared to wild-type PrV was observed on human 143TK⁻ cells (Fig. 2, lower panel). Remarkably, this is the cell line used for successful isolation of UL20⁻ HSV-1 mutants (3). Plaque sizes of the UL20 rescue mutant PrV UL20R were similar to that of wild type or PrV-1112 on complementing as well as on noncomplementing cell lines (data not shown).

In addition, one-step growth kinetics of PrV ΔUL20Z, PrV UL20R, and wild-type PrV were compared on Vero and VneoB4 cells (Fig. 3). The cells were infected at a multiplicity of infection (MOI) of 5. After 1 h at 4°C, prewarmed medium was added, and the cells were further incubated for 1 h at 37°C to allow virus penetration. After this time, the inoculum was removed, remaining extracellular virus was inactivated by low pH, and cells were overlaid with fresh medium. Immediately thereafter, and after 4, 8, 12, 24, 36, and 48 h of incubation at 37°C, adherent cells were scraped into the medium. Cells were then separated from released virions by centrifugation for 10 min at 2,500 × *g*, resuspended in the same volume of fresh medium, and subjected to one freezing (−70°C) and thawing (37°C) cycle. Plaque assays of both intracellular and released virions were performed on complementing VneoB4 cells to provide equal growth conditions for wild-type and mutant virus. Infectious progeny virus was first detected 8 h after infection of either cell line with the wild type or with PrV ΔUL20Z, indicating that virus entry and replication are not significantly impaired in the absence of the UL20 gene product. Increasing amounts of cell-associated infectivity were found in Vero and VneoB4 cells (Fig. 3A and C) up to 12 h after infection. In contrast, maximum titers of released virions in the medium (Fig. 3B and D) were not observed before 24 to 36 h postinfection. Whereas the overall time course of virus propagation in Vero cells infected with either wild-type or UL20⁻ PrV appears similar, final titers diverge significantly (Fig. 3A and B). Compared to wild-type PrV, maximum intracellular titers of PrV ΔUL20Z were decreased approximately 10-fold, whereas infectivity in the supernatant showed an approximately 100-fold reduction. Wild-type-like titers of both intracellular and extracellular virus were obtained after restoration of the UL20 gene in PrV UL20R propagated on Vero cells (Fig. 3A and B), as well as by propagation of PrV ΔUL20Z on cell line VneoB4 (Fig. 3C and D).

Taken together, the data obtained from plaque assays and

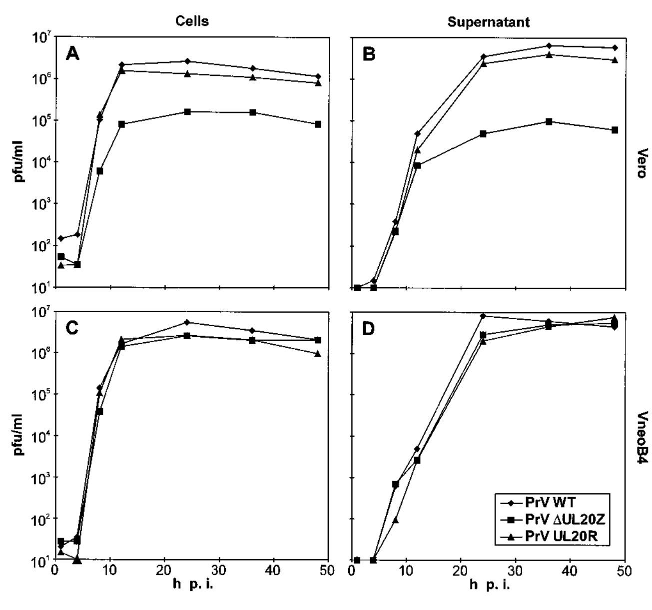

FIG. 3. One-step growth curves of UL20⁻ PrV. Vero and VneoB4 cells were infected with either wild-type PrV (WT), PrV recombinant ΔUL20Z, or rescue mutant UL20R at an MOI of 5 for 1 h at 4°C. After an additional hour at 37°C, nonpenetrated virus was inactivated by low-pH treatment. Immediately thereafter, and after indicated periods of incubation at 37°C, cells and supernatants were harvested separately, and progeny virus titers were determined on VneoB4 cells.

one-step growth kinetics point to an impairment of cell-to-cell spread and release of UL20^{-} PrV, which can be compensated for by the intact UL20 gene in *trans*. It appears unlikely that the defects of PrV ΔUL20Z are caused by mutations other than the inactivation of the UL20 gene, since the affected ORF does not overlap with any other known viral gene and is presumably expressed from a monocistronic mRNA (20). Furthermore, PrV ΔUL20Z could be rescued in *cis* to a wild-type-like phenotype with a cloned DNA fragment which contains the intact PrV UL20 gene flanked only by the 5′-terminal part of UL19 and the UL21 ORF (Fig. 1C). Both PrV UL19 and UL21 encode viral capsid proteins (12, 20) which are involved in intranuclear capsid formation. Electron microscopic studies (see below) of noncomplementing Vero cells infected with PrV ΔUL20Z, however, did not reveal any impairment of nucleocapsid assembly.

Macroscopically, the egress defect of UL20^{-} PrV on Vero cells was found to be similar, although less striking, than that of a UL20^{-} HSV-1 mutant on the same cell line (3). Similar to the HSV-1 mutant, plaque formation of PrV ΔUL20Z was also impaired to a different extent on various noncomplementing cell lines. Remarkably, the effect of both HSV and PrV UL20 mutations was most pronounced in Vero cells and least in human 143TK^{-} cells. In HSV-1, this finding correlates with a fragmentation of the Golgi apparatus observed at late times after infection of Vero cells but not of 143TK^{-} cells (9). Therefore, it was concluded that the HSV-1 UL20 protein compensates for the disruption of the cellular exocytosis pathway and thereby permits viral egress (1). PrV might influence host cell organization in a similar manner, which could explain the observation that at early times after infection (up to 12 h) PrV ΔUL20Z was released from Vero cells nearly as efficiently as wild-type PrV.

Ultrastructural studies were performed to pinpoint the defect in maturation and egress of UL20^{-} PrV. To this end, Vero and VneoB4 cells were infected with either wild-type PrV or PrV ΔUL20Z at an MOI of 5 and incubated at 37°C for 14 h. This was the earliest time after infection at which the UL20^{-} mutant exhibited a pronounced replication defect (Fig. 3). Ultrathin sections of fixed cells were prepared as described previously (14) and examined with a transmission electron microscope (EM400T; Philips, Eindhoven, The Netherlands). Wild-type PrV-infected Vero or VneoB4 cells (data not shown) showed typical stages of herpesvirus maturation, including the assembly of nucleocapsids in the nucleus, primary envelopment at the inner nuclear membrane, secondary envelopment of intracytoplasmic nucleocapsids in the Golgi region, and release of enveloped virions from the cells (17). Maturation of PrV ΔUL20Z was found to be similar to that of wild-type PrV in transcomplementing VneoB4 cells (Fig. 4). Budding of cytoplasmic virions into vesicles (Fig. 4C, arrowheads and insets) was observed, and enveloped particles were released efficiently from the cells (Fig. 4A and B). In normal Vero cells infected with PrV ΔUL20Z (Fig. 5), the nuclear stages of virus maturation as well as transit through the nuclear membrane were not affected (Fig. 5A and B), and budding of nucleocapsids into cytoplasmic vesicles was detected frequently (Fig. 5C, arrows and insets). These vesicles were presumably derived from the Golgi apparatus, since they were clearly separated from nuclear membranes and located adjacent to Golgi cisternae (Fig. 5A) (17). The membrane projections of the budding virions (Fig. 5C, arrowheads in insets), which probably represent viral glycoproteins, are typical for secondary envelopes acquired during budding into vesicles in the *trans*-Golgi area (17). In contrast to the situation in complementing cells, however, enveloped particles of UL20^{-} PrV apparently accumulated in these vesicles, leading to an enlargement of the vacuoles (Fig. 5), and only very few extracellular virions were detectable.

To quantify the observed differences, virus particles localized in distinct compartments of either Vero or VneoB4 cells infected with PrV ΔUL20Z were counted in randomly selected electron micrographs of 10 cells each and the subcellular distribution of virions was determined (Table 1). In both cell types, nearly 50% of the virus particles were found in the nuclei, but only a few of them were localized in the perinuclear space. The proportion of naked PrV ΔUL20Z nucleocapsids appeared to be slightly increased in the cytoplasm of Vero cells. However, the most striking observation was an approximately 10-fold increase in the proportion of enveloped particles found within cytoplasmic vesicles. This correlates with a decrease in the number of detectable extracellular virions. Ultrastructural analyses at different time points after infection (data not shown) indicated that intracellular virion maturation of UL20^{-} PrV did not differ significantly between Vero and VneoB4 cells up to 8 h after infection, which correlates with the results from replication kinetics (Fig. 3). The data also show that all stages of virion maturation are detectable at the chosen time point of 14 h after infection. Only cells which demonstrated no gross destructive changes in cell morphology were analyzed (Fig. 4 and 5). These findings demonstrate that morphogenesis of UL20^{-} PrV virions proceeds past the secondary envelopment stage and is blocked prior to exocytosis of enveloped intravesicular virions. Thus, PrV UL20 protein appears to function in a different cellular compartment compared to HSV-1 UL20.

Taken together, our results indicate that in the absence of functional UL20 gene product of PrV a very late step of virus egress, presumably transport of secondary enveloped virions to the cell surface, is severely impaired. This finding clearly differs from observations of UL20^{-} HSV-1, which was shown to be retained after primary envelopment in the perinuclear space

TABLE 1. Intracellular distribution of virus particles[a]

Localization	Vero cells	Avg particle no. (% of particles/cell)	VneoB4 cells	Avg particle no. (% of particles/cell)
Nucleus	26, 32, 43, 51, 18, 20, 27, 23, 14, 30	28.4 (43.6)	34, 18, 54, 41, 63, 32, 47, 21, 15, 38	36.3 (45.8)
Perinuclear space	1, 0, 0, 2, 0, 1, 4, 2, 0, 4	1.4 (2.2)	1, 0, 0, 0, 3, 0, 0, 1, 0, 4	0.9 (1.1)
Golgi region (unenveloped)	15, 14, 9, 10, 12, 1, 4, 15, 17, 8	10.5 (16.1)	9, 4, 8, 11, 6, 2, 0, 7, 13, 0	6.0 (7.6)
Golgi region (enveloped)	25, 18, 16, 19, 29, 16, 26, 42, 31, 12	23.4 (35.9)	3, 6, 5, 2, 7, 1, 4, 0, 0, 2	3.0 (3.7)
Extracellular particles	0, 0, 3, 4, 1, 0, 0, 0, 6, 0	1.4 (2.1)	12, 18, 36, 29, 38, 28, 17, 26, 13, 31	24.8 (31.3)
Total particle no./cell	67, 64, 71, 86, 60, 38, 61, 82, 68, 54	65.1	59, 46, 103, 83, 117, 63, 68, 55, 41, 75	79.3

[a] Numbers of virus particles present in the different compartments of UL20^{-} PrV-infected Vero and VneoB4 cells were determined. Particles were counted in electron micrographs of 10 randomly selected cells of each line. The average particle numbers in each compartment and the relative abundance compared to total number of particles (% of particles per cell) were determined.

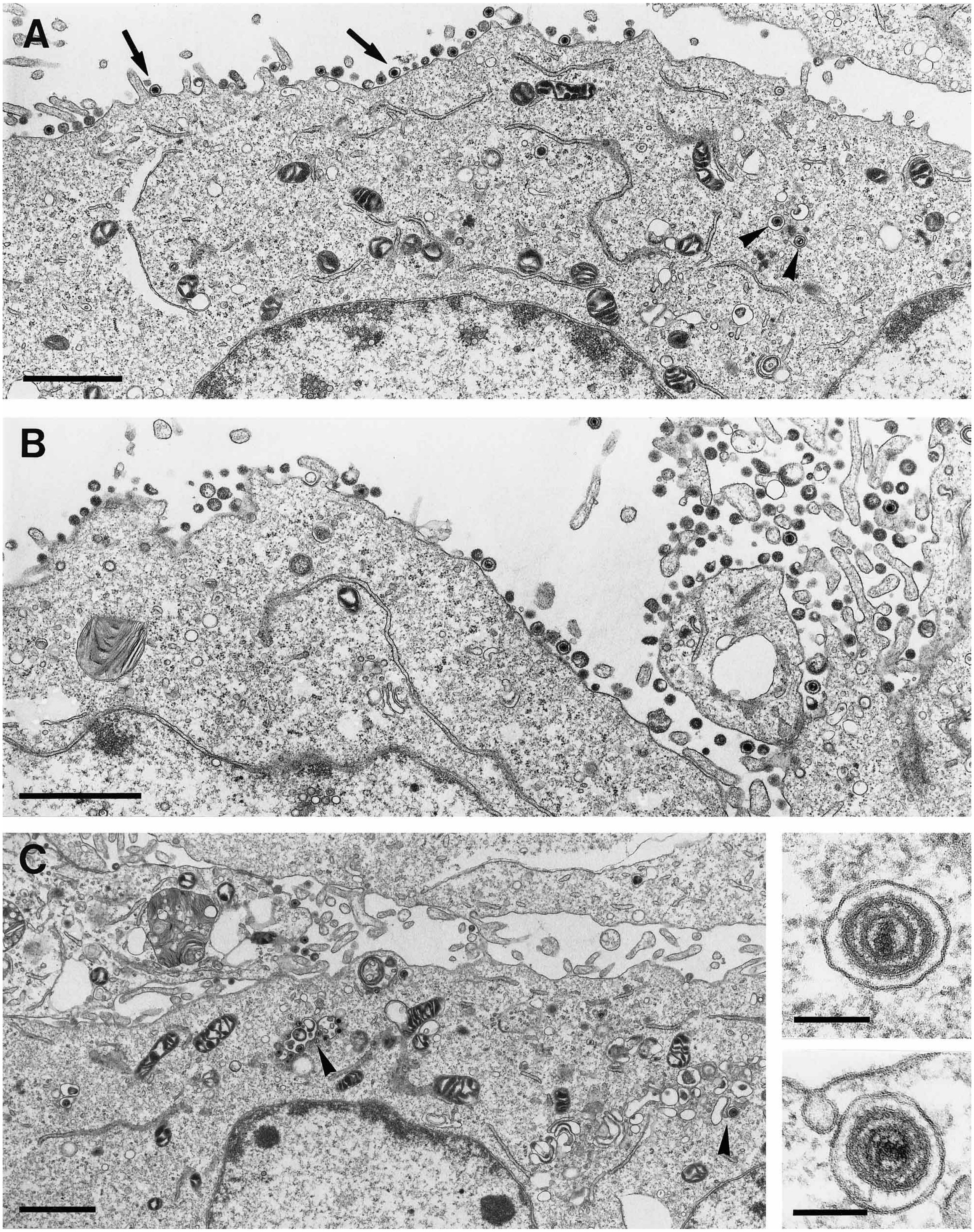

FIG. 4. Electron microscopy of UL20⁻ PrV-infected VneoB4 cells. Cells were analyzed 14 h after infection with PrV ΔUL20Z at an MOI of 5. Bars represent 1.5 μm in panels A and B, 1.0 μm in panel C, and 150 nm in the insets. Enveloped virus particles in cytoplasmic vesicles are marked by arrowheads in panel A and are also depicted at a higher magnification in the insets in panel C. Arrowheads in panel C mark particles during budding into vesicles. Extracellular virions are indicated by the arrows in panel A.

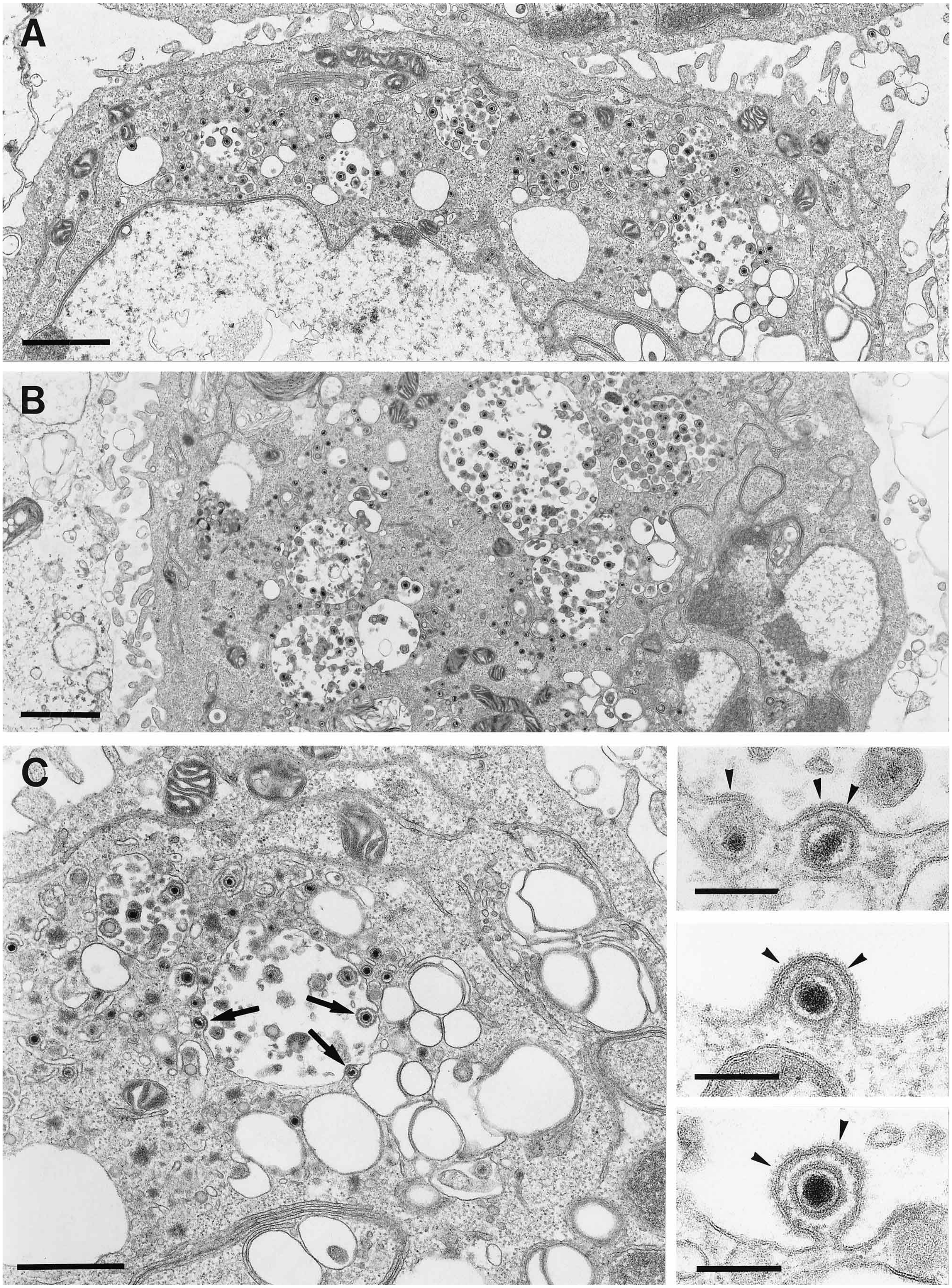

FIG. 5. Electron microscopy of UL20^{-} PrV-infected Vero cells. Investigations were performed 14 h after infection with PrV ΔUL20Z at an MOI of 5. Bars represent 1.5 μm in panels A and B, 1.0 μm in panel C, and 150 nm in the insets. Arrows denote particles in the budding process shown at a higher magnification in the insets. Arrowheads indicate surface projections of virion envelopes during and after budding into cytoplasmic vesicles. Note the accumulation of enveloped particles in these vesicles and the absence of extracellular virions in Vero cells infected with PrV ΔUL20Z.

between the inner and outer nuclear membranes of Vero cells (1, 3). The different blocks in egress of HSV-1 and PrV UL20 gene mutants might be explained by distinct functions of the UL20 proteins, correlating with their limited degree of amino acid sequence conservation, amounting to only 33% (20).

The differences between the intracellular phenotypes of the UL20 mutants could also be due to generally different pathways of egress in HSV and PrV. Egress of HSV-1 is proposed to occur by envelopment at the inner nuclear membrane followed by transit of enveloped virions through the endoplasmatic reticulum and the Golgi apparatus, where envelope glycoproteins are processed to their mature forms (32). The occasional appearance of naked nucleocapsids in the cytoplasm of infected cells was considered to be accidental (8). In contrast, studies with PrV (17, 35, 36) and VZV (15) indicated that the release of nucleocapsids from the outer nuclear membrane or from the endoplasmic reticulum to the cytoplasm is a general step of viral egress, followed by secondary envelopment in the *trans*-Golgi region. Recently, we characterized a PrV mutant which is impaired in secondary envelopment, leading to an accumulation of naked nucleocapsids in the Golgi region of infected Vero cells (14). This defect is caused by the deletion of the viral UL3.5 gene (11) and could be complemented in *trans* on a PrV UL3.5-expressing Vero cell line. Remarkably, the UL3.5 gene is not conserved in the genome of HSV-1 (24), correlating with the described differences in virion maturation. Egress of the PrV UL20 mutant described in the present study appears impaired after secondary envelopment in the *trans*-Golgi region has occurred. From our findings, we conclude that the UL20 gene product of PrV is required for release of terminally enveloped virions from cells, in which the natural exocytosis pathways are disrupted. Thus, assuming that HSV-1 acquires its immature but final envelope already at the inner nuclear membrane (32), PrV and HSV-1 UL20 functions could be considered to be similar in that they play a role in transcellular transport of enveloped virions. However, both act in different intracellular compartments.

Besides affecting exocytosis of virus particles, HSV-1 UL20 was also shown to contribute to transport and processing of viral glycoproteins (1). Preliminary analyses revealed no obvious alterations in content and maturation of viral glycoproteins in cells infected with PrV ΔUL20Z compared to wild-type PrV (data not shown). However, more detailed studies are required to analyze the subcellular distribution of viral glycoproteins as well as their maturation grade in virion envelopes of $UL20^-$ PrV.

At present, the molecular mechanism of UL20 function is unclear, and localization of the PrV UL20 protein has failed up to now due to a lack of proper immunological reagents. However, our experimental system consisting of defined PrV mutants impaired at different stages of virion maturation provides a promising basis for a more detailed understanding of the complex process of herpesvirus egress.

This study was supported by a grant from the Deutsche Forschungsgemeinschaft (Me 854/3).

We thank C. Ehrlich and C. Möller for expert technical assistance.

REFERENCES

1. **Avitabile, E., P. L. Ward, C. Di Lazzaro, M. R. Torrisi, B. Roizman, and G. Campadelli-Fiume.** 1994. The herpes simplex virus UL20 protein compensates for the differential disruption of exocytosis of virions and viral membrane glycoproteins associated with fragmentation of the Golgi apparatus. J. Virol. **68:**7397–7405.
2. **Babic, N., T. C. Mettenleiter, G. Ugolini, A. Flammand, and P. Coulon.** 1994. Propagation of pseudorabies virus in the nervous system of the mouse after intranasal inoculation. Virology **204:**616–625.
3. **Baines, J. D., P. L. Ward, G. Campadelli-Fiume, and B. Roizman.** 1991. The U_L20 gene of herpes simplex virus 1 encodes a function necessary for viral egress. J. Virol. **65:**6414–6424.
4. **Baines, J. D., A. Koyama, T. Huang, and B. Roizman.** 1994. The U_L21 gene products of herpes simplex virus 1 are dispensable for growth in cultured cells. J. Virol. **68:**2929–2936.
5. **Baumeister, J., B. G. Klupp, and T. C. Mettenleiter.** 1995. Pseudorabies virus and equine herpesvirus 1 share a nonessential gene which is absent in other herpesviruses and located adjacent to a highly conserved gene cluster. J. Virol. **69:**5560–5567.
6. **Ben-Porat, T., R. A. Veach, and S. Ihara.** 1983. Localization of the regions of homology between the genomes of herpes simplex virus type 1 and pseudorabies virus. Virology **127:**194–204.
7. **Ben-Porat, T., and A. S. Kaplan.** 1985. Molecular biology of pseudorabies virus, p. 105–173. *In* B. Roizman (ed.), The herpesviruses, vol. 3. Plenum Publishing Corp., New York, N.Y.
8. **Campadelli-Fiume, G., F. Farabegoli, S. Di Gaeta, and B. Roizman.** 1991. Origin of unenveloped capsids in the cytoplasm of cells infected with herpes simplex virus 1. J. Virol. **65:**1589–1595.
9. **Campadelli-Fiume, G., R. Brandimarti, C. Di Lazzaro, P. L. Ward, B. Roizman, and M. R. Torrisi.** 1993. Fragmentation and dispersal of Golgi proteins and redistribution of glycoproteins and glycolipids processed through the Golgi apparatus after infection with herpes simplex virus 1. Proc. Natl. Acad. Sci. USA **90:**2798–2802.
10. **Davison, A. J., and J. E. Scott.** 1986. The complete DNA sequence of varicella-zoster virus. J. Gen. Virol. **67:**1759–1816.
11. **Dean, H. J., and A. K. Cheung.** 1993. A 3′ coterminal gene cluster in pseudorabies virus contains herpes simplex virus UL1, UL2, and UL3 gene homologs and a unique UL3.5 open reading frame. J. Virol. **67:**5955–5961.
12. **de Wind, N., F. Wagenaar, J. Pol, T. Kimman, and A. Berns.** 1992. The pseudorabies virus homolog of the herpes simplex virus UL21 gene product is a capsid protein which is involved in capsid maturation. J. Virol. **66:**7096–7103.
13. **Dezélée, B., F. Bras, P. Vende, B. Simonet, X. Nguyen, A. Flamand, and M. J. Masse.** 1996. The Bam HI fragment 9 of pseudorabies virus contains genes homologous to the UL24, UL25, UL26, and UL26.5 genes of herpes simplex virus type 1. Virus Res. **42:**27–39.
14. **Fuchs, W., B. G. Klupp, H. Granzow, H.-J. Rziha, and T. C. Mettenleiter.** 1996. Identification and characterization of the pseudorabies virus UL3.5 protein, which is involved in virus egress. J. Virol. **70:**3517–3527.
15. **Gershon, A. A., D. L. Sherman, Z. Zhu, C. A. Gabel, R. T. Ambron, and M. D. Gershon.** 1994. Intracellular transport of newly synthesized varicella-zoster virus: final envelopment in the *trans*-Golgi network. J. Virol. **68:**6372–6390.
16. **Graham, F. L., and A. J. van der Eb.** 1973. A new technique for the assay of infectivity of human adenovirus. Virology **52:**456–467.
17. **Granzow, H., F. Weiland, A. Jöns, B. G. Klupp, A. Karger, and T. C. Mettenleiter.** 1997. Ultrastructural analysis of the replication cycle of pseudorabies virus in cell culture: a reassessment. J. Virol. **71:**2072–2082.
18. **Kaplan, A. S., and A. E. Vatter.** 1959. A comparison of herpes simplex and pseudorabies viruses. Virology **7:**394–407.
19. **Klupp, B. G., and T. C. Mettenleiter.** 1991. Sequence and expression of the glycoprotein gH gene of pseudorabies virus. Virology **182:**732–741.
20. **Klupp, B. G., H. Kern, and T. C. Mettenleiter.** 1992. The virulence-determining genomic BamHI fragment 4 of pseudorabies virus contains genes corresponding to the UL15 (partial), UL18, UL19, UL20, and UL21 genes of herpes simplex virus and a putative origin of replication. Virology **191:** 900–908.
21. **Klupp, B. G., N. Visser, and T. C. Mettenleiter.** 1992. Identification and characterization of pseudorabies virus glycoprotein H. J. Virol. **66:**3048–3055.
22. **Klupp, B. G., B. Lomniczi, N. Visser, W. Fuchs, and T. C. Mettenleiter.** 1995. Mutations affecting the UL21 gene contribute to avirulence of pseudorabies virus vaccine strain Bartha. Virology **212:**466–473.
23. **MacLean, C. A., S. Efstathiou, M. L. Elliott, F. E. Jamieson, and D. J. McGeoch.** 1991. Investigation of herpes simplex virus type 1 genes encoding multiply inserted membrane proteins. J. Gen. Virol. **72:**897–906.
24. **McGeoch, D. J., M. A. Dalrymple, A. J. Davison, A. Dolan, M. C. Frame, D. McNab, L. J. Perry, J. E. Scott, and P. Taylor.** 1988. The complete DNA sequence of the unique long region in the genome of herpes simplex virus type 1. J. Gen. Virol. **69:**1531–1574.
25. **Mettenleiter, T. C.** 1994. Pseudorabies (Aujeszky's disease) virus: state of the art. Acta Vet. Hung. **42:**153–177.
26. **Mettenleiter, T. C., and I. Rauh.** 1990. A glycoprotein gX-β-galactosidase fusion gene as insertional marker for rapid identification of pseudorabies virus mutants. J. Virol. Methods **30:**55–66.
27. **Mettenleiter, T. C., H. Kern, and I. Rauh.** 1990. Isolation of a viable herpesvirus (pseudorabies virus) mutant specifically lacking all four known nonessential glycoproteins. Virology **179:**498–503.
28. **Roizman, B., R. Derosiers, B. Fleckenstein, C. Lopez, A. C. Minson, and M. J. Studdert.** 1992. The family Herpesviridae: an update. Arch. Virol. **123:**425–449.
29. **Sanes, J., J. Rubenstein, and J.-F. Nicolas.** 1986. Use of recombinant ret-

rovirus to study post-implantation cell lineage in mouse embryos. EMBO J. **5:**3133–3142.
30. **Schwyzer, M., and M. Ackermann.** 1996. Molecular virology of ruminant herpesviruses. Vet. Microbiol. **53:**17–29.
31. **Telford, E. A., M. S. Watson, K. McBride, and A. J. Davison.** 1992. The DNA sequence of equine herpesvirus-1. Virology **189:**304–316.
32. **Torrisi, M. R., C. Di Lazzaro, A. Pavan, L. Pereira, and G. Campadelli-Fiume.** 1992. Herpes simplex virus envelopment and maturation studied by fracture label. J. Virol. **66:**554–561.
33. **Vlcek, C., V. Benes, Z. Lu, G. F. Kutish, V. Paces, D. Rock, G. Letchworth, and M. Schwyzer.** 1995. Nucleotide sequence analysis of a 30-kb region of the bovine herpesvirus 1 genome which exhibits a colinear gene arrangement with the UL21 to UL4 genes of herpes simplex virus. Virology **210:**100–108.
34. **Ward, P. L., G. Campadelli-Fiume, E. Avitabile, and B. Roizman.** 1994. Localization and putative function of the U_L20 membrane protein in cells infected with herpes simplex virus 1. J. Virol. **68:**7406–7417.
35. **Whealy, M. E., J. P. Card, R. P. Meade, A. K. Robbins, and L. W. Enquist.** 1991. Effect of brefeldin A on alphaherpesvirus membrane protein glycosylation and virus egress. J. Virol. **65:**1066–1081.
36. **Whealy, M. E., A. K. Robbins, F. Tufaro, and L. W. Enquist.** 1992. A cellular function is required for pseudorabies virus envelope glycoprotein processing and virus egress. J. Virol. **66:**3803–3810.
37. **Wittmann, G., and H.-J. Rziha.** 1989. Aujeszky's disease (pseudorabies) in pigs, p. 230–325. *In* G. Whittmann (ed.), Herpes diseases of cattle, horses and pigs. Kluver, Boston, Mass.